

## **AuNPs-capped cage fluorescent biosensor based on controlled-release and cyclic enzymatic amplification for ultrasensitive detection of ATP**

Wei Wang,\* Xin Li, Kai Tang, Zhiling Song, and Xiliang Luo\*

Key Laboratory of Optic-electric Sensing and Analytical Chemistry for Life Science, Ministry of Education, Shandong Key Laboratory of Biochemical Analysis, Key Laboratory of Analytical Chemistry for Life Science in Universities of Shandong, College of Chemistry and Molecular Engineering, Qingdao University of Science and Technology, Qingdao, 266042, P. R. China

### **Characterization of the synthesized AuNCs**

UV-visible-near-IR absorbance spectrum of AuNCs (**Figure. S1**) is proved here to exhibit its surface plasmon resonance peak.

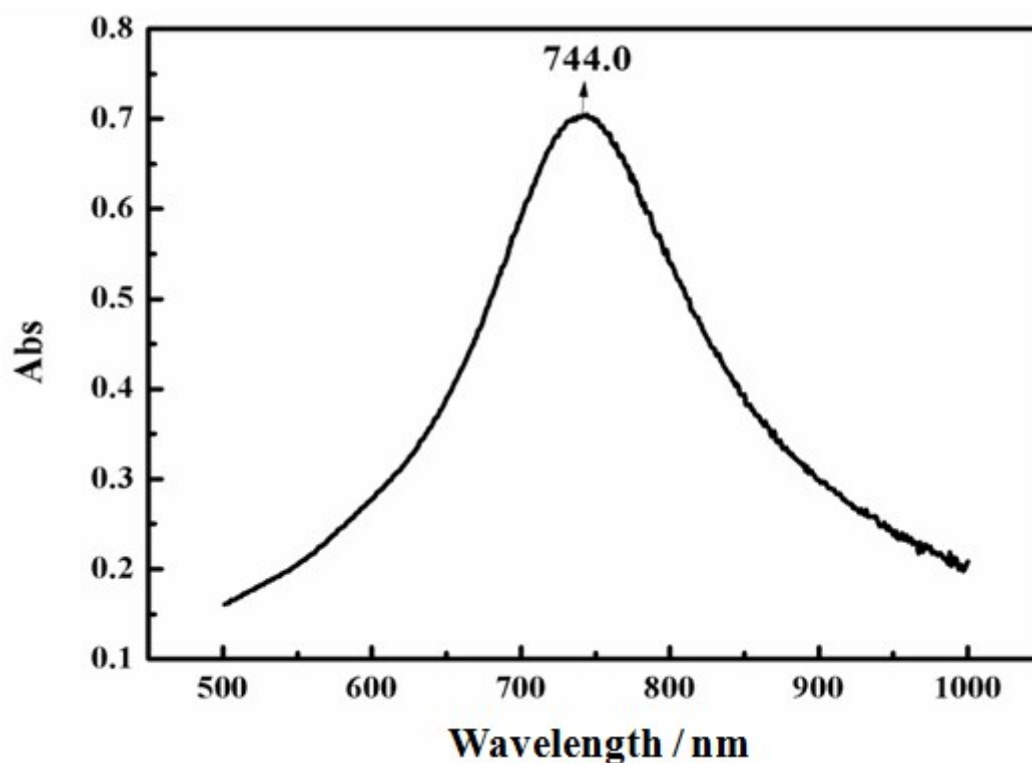


**Figure. S1** UV-visible-near-IR absorbance spectrum of AuNCs.

### **Characterization of the synthesized AuNPs**

UV-visible-near-IR absorbance spectrum of AuNPs (**Figure. S2**) is proved here to exhibit its absorption peak.

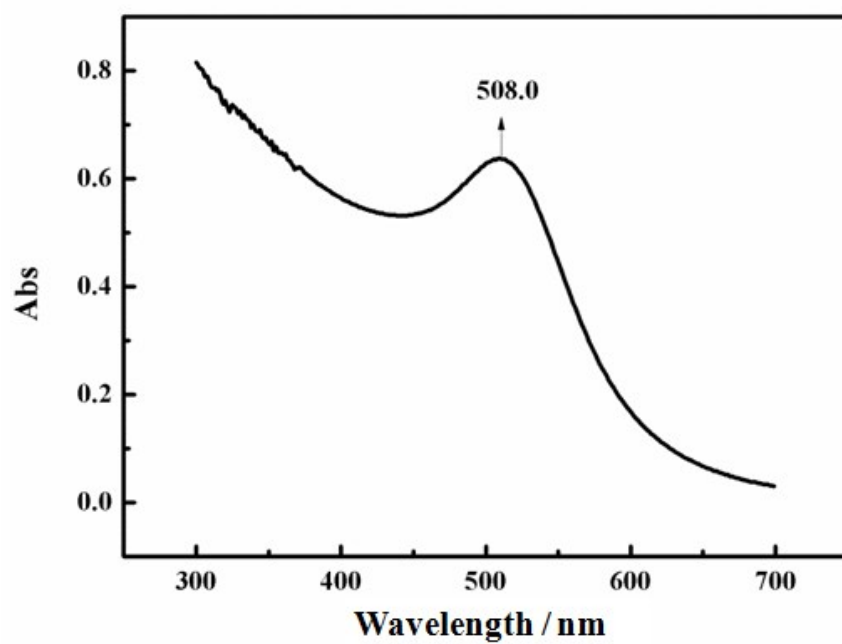


**Figure. S2** UV-visible-near-IR absorbance spectrum of AuNPs.

**TEM image of the synthesized AuNPs-capped AuNCs.**

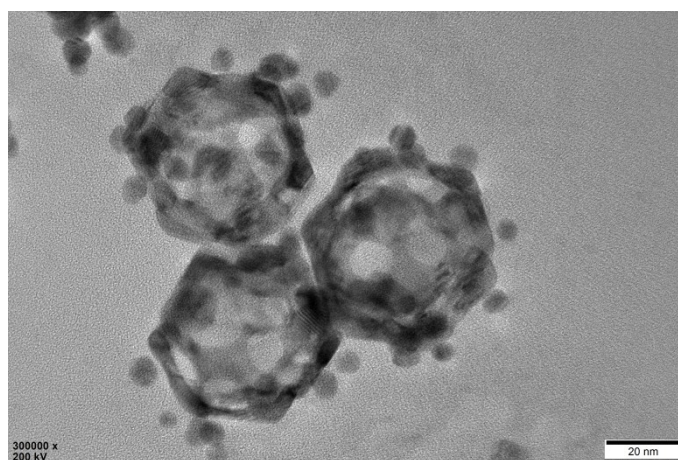


**Figure. S3** TEM image of the synthesized AuNPs-capped AuNCs.

### Optimization of the incubation temperature

**Figure. S4** showed the different fluorescence signals of the sensing system in the presence of the  $1.0 \times 10^{-7}$  M ATP at different temperature.

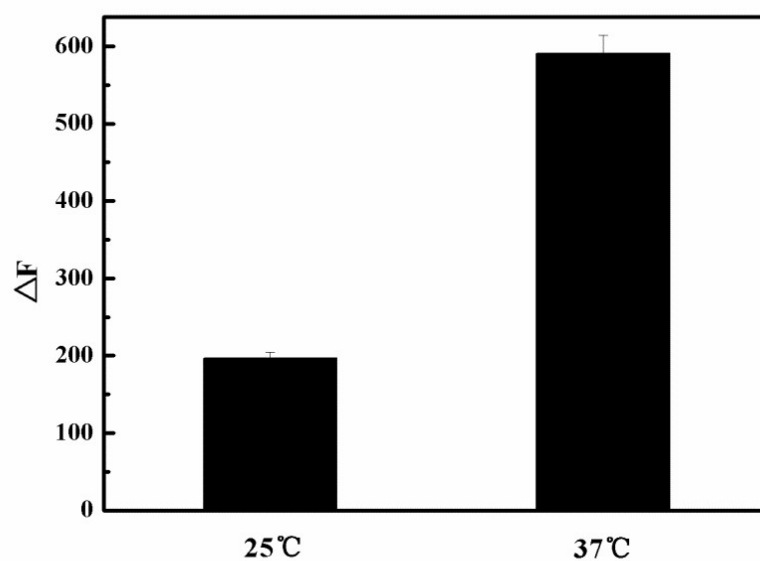


**Figure. S4** The different fluorescence signals between ExoIII reaction with the corresponding blank at different temperature.

### Optimization of the reaction time

**Figure. S5** showed the relationship between the reaction time and the fluorescence of the RhB in the presence of the  $1.0 \times 10^{-7}$  M ATP.

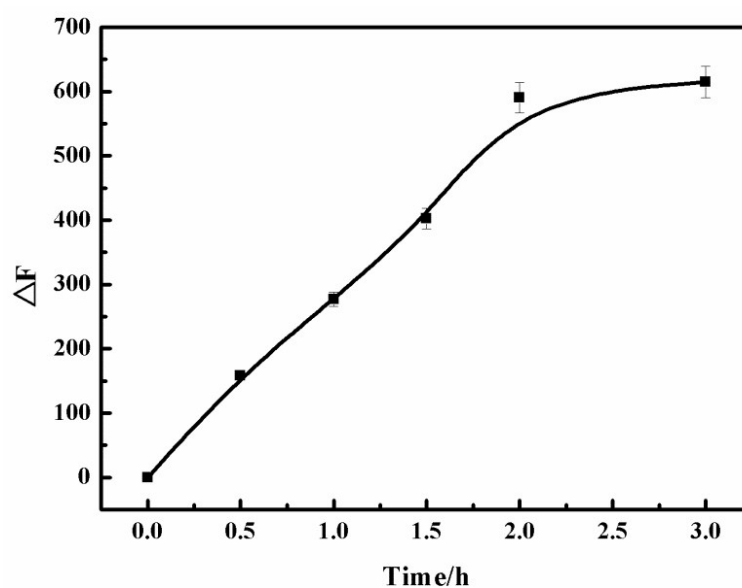


**Figure. S5** The relationship between the reaction time and the fluorescence of the RhB in the presence of the  $1.0 \times 10^{-7}$  M ATP.

### Preliminary analysis of the biosensor in tumor cells

**Fig S6** showed the fluorescence intensity of RhB from the hollow interiors of AuNCs toward Hela cell lysate (curve a) and PBS (curve b).

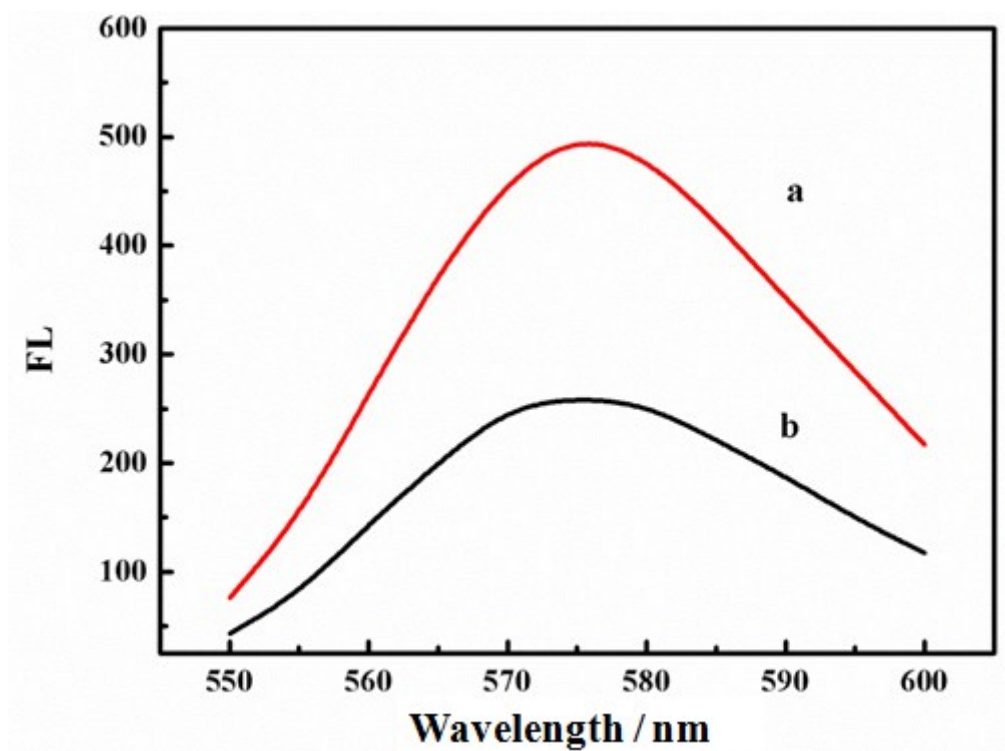


**Fig. S6** The fluorescent signal of RhB released from the hollow interiors of AuNCs toward Hela cells lysate (a) and PBS (b).

Table. S1 Comparison of different methods for assay of ATP.

Methods	Detection Limit	Linear Range	Refs
Ratiometric biosensor	1.3 $\mu\text{M}$	0 – 150 $\mu\text{M}$	[1]
Fluorescent sensor	42.3 nM	0 – 20 $\mu\text{M}$	[2]
GSH-AuNCs complex	1 $\mu\text{M}$	0 – 100 $\mu\text{M}$	[3]
Fluorescent probe	5 $\mu\text{M}$	0 – 140 $\mu\text{M}$	[4]
DNAzyme amplification	150 nM	2 – 90 $\mu\text{M}$	[5]
G-quadruplex sensor	3.5 $\mu\text{M}$	10 – 50 $\mu\text{M}$	[6]
Ratiometric sensor	65 nM	0.1 – 10 $\mu\text{M}$	[7]
GO-allosteric aptasensor	31 nM	50 – 500 nM	[8]
Fluorescent biosensor	0.88 nM	1 – 100 nM	This work

## References

- [1] V. R. Singh and P. K. Singh, *J. Mater. Chem. B*, 2020, **8**, 1182-1190.
- [2] L. Y. Geng, Y. Zhao, E. Kamy, J. T. Guo, B. Sun, Y. K. Feng, M. F. Zhu and X. K. Ren, *J. Mater. Chem. C*, 2019, **7**, 2640-2645.

- [3] J. G. You, C. Y. Lu, A. S. Krishna Kumar and W. L. Tseng, *Nanoscale*, 2018, **10**, 17691-17698.
- [4] Y. Zhong and T. Yi, *J. Mater. Chem. B*, 2019, **7**, 2549-2556.
- [5] F. Gao, J. Wu and Y. Yao, *RSC Advances*, 2018, **8**, 28161-28171.
- [6] S. Srinivasan, V. Ranganathan, M. C. DeRosa and B. M. Murari, *Anal. Bioanal. Chem.*, 2019, **411**, 1319-1330.
- [7] S. Yao, Y. Gao and W. Wang, *Analytical Methods*, 2017, **9**, 3244-3248.
- [8] S. He, L. Qu and Y. Tan, *Analytical Methods*, 2017, **9**, 4837-4842.